

The Application of Microchannel Heat Sinks With Triangle Ribs for Thermal Management

Fadi Alnaimat

Mechanical Engineering Department, United Arab Emirates University, Al Ain, Abu Dhabi, UAE

ABSTRACT

A microchannel heat sink with a smooth and triangle-ribs embedded surface is examined using a simulation-based study. The heat sink is composed of microchannels, each of which is 1 cm long and 150 μ m wide. The heat sink is studied using water. A range of Reynolds numbers, from 100 to 500, are used in the study. The thermal performance is computed using the fluids' surface temperatures as well as the fluid inlet and exit temperatures. The analysis found that a greater Reynolds number increases the Nusselt number and the heat transfer coefficient. It has also been observed that the friction factor decreases as the Reynolds number increases. The heat transmission rate of the triangle-ribs microchannel was clearly higher than that of the smooth one. The total friction factor of the heat sink with triangle-rib microchannels is also found to be higher than that of the heat sink with smooth channels. Furthermore, it is noticed in the obtained results that as the Reynolds number rises, the pressure drop rises.

Keywords: Microchannels, Heat sink, Pin fins

INTRODUCTION

Heat transfer devices of all sizes are increasingly using microchannels, which are typically defined as flow tunnels with a hydraulic diameter of less than $1000~\mu m$ (Mathew & Weiss, 2015). Improved surface area density and an enhanced heat transfer coefficient are two benefits of microchannels that can result in either a decrease in the device's volume for the same heat duty or an increase in the device's heat duty for the same volume (Mathew & Weiss, 2015). Even now, efforts are being made to increase the heat transmission coefficient in microchannels. The heat transfer coefficient in microchannels can be increased passively using a variety of methods. Passive approaches frequently include altering or partially limiting flow paths.

The performance of the microchannel, a passive method of improving heat transmission, has been better understood by studying a variety of variants (Zheng et al., 2013.a; 2013.b). The zigzag microchannel itself, two sidewalls, and the bottom wall are the only three walls that experience a continuous heat flux. Sui et al. (2010) investigated the performance of wavy microchannels in laminar flow numerically. They investigated three distinct

cases: conjugate heat transfer, constant temperature, and constant heat flux. Each case's performance was contrasted with that of a straight microchannel in comparable circumstances. Zheng et al. (2013.a) investigated the thermohydraulic performance of a microchannel with a square cross-section and rounded corners with constant heat flux. Daadoua et al. (2024) and Alnaimat et al. (2020) are two studies that investigated heat transfer enhancement by experimental testing on minichannels. Applications for microchannels in heat transfer are numerous (El Kadi et al., 2021; Alnaimat et al., 2023).

Microchannels with smooth and another triangle sidewall ribs, as shown in Figure 1, are the subject of this study. The two sidewalls of the microchannel distribute the heat flux. The friction factor and Nusselt number are used to assess the microchannel's performance. The performance of a microchannel will be examined in this study in connection to its Reynolds number. The channels have a width of 150 μ m and a length of 1 cm. Two distinct microchannels, one standard smooth channel, and another with triangle ribs (20 μ m base and 20 μ m height) were investigated. One millimeter separates each rib. This analysis assumes that the flow is uniform in all channels, even though several works by Alnaimat et al. (2023) explore the impact of the manifold on the flow maldistribution.

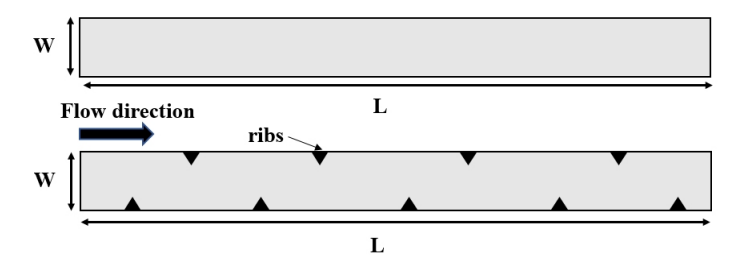


Figure 1: Schematic of microchannel view smooth and triangle ribs indicating dimensions and flow direction.

MATHMATICAL MODEL

A mathematical model is used to describe the microchannel shown in Figure 1. The Navier-Stokes equations, the continuity equation, and the energy equation make up this system. According to Alnaimat et al. (2024), Equation (1) represents the continuity equation, Equation (2) represents the Navier-Stokes equations, and Equation (3) represents the energy equation.

$$\nabla \cdot \mathbf{V}_f = 0 \tag{1}$$

$$\rho_f \mathbf{V}_f \cdot \nabla \mathbf{V}_f = -\nabla P_f + \mu_f \nabla^2 \mathbf{V}_f \tag{2}$$

$$\rho_f C_{p,f} \mathbf{V}_f \cdot \nabla T_f = k_f \nabla^2 T_f \tag{3}$$

2200 Alnaimat

Where V_f (m/s) is the fluid velocity vector, P_f (Pa) is the pressure of the fluid, T_f (K) represents the temperature of the fluid, μ_f (Pa.s) is the fluid viscosity, ρ_f (kg/m³) represent the fluid density, k_f (W/mK) is the fluid thermal conductivity and $C_{p,f}$ (J/kgK) is the fluid specific heat capacity. The flow is assumed to be Laminar in the microchannel, and negligible heat loss between the microchannel and the surrounding environment, and negligible viscous heat transfer.

A mathematical modeling method similar to that outlined by Alnaimat et al. (2022; 2024; 2025) is used to establish the modeling for this work. The following are examples of boundary conditions for the model: Equation (4) indicates that the microchannel's inlet has a specific velocity; its temperature at the inlet is specified, i.e., $T_{f,in}=293~\rm K$; its walls have no-slip flow conditions; its outlet has zero gauge pressure, or $P_{f,out}=0$; Equation (5) indicates that the microchannel's top wall and outlet are adiabatic; and its two sidewalls are subjected to a constant heat flux.

$$V_{f,in} = Re\mu_f/\rho_f D_{hv} \tag{4}$$

$$q'' = 200,000 \frac{W}{m^2} \tag{5}$$

Where Re is the Reynold number, D_{hy} is the hydraulic diameter of the microchannel and q'' is the heat flux applied to the walls. Ansys Workbench's Fluent module is used to run the simulation. This work makes use of the SIMPLE algorithm. Equations (6) and (7) are used to produce the friction factor and Nusselt number, respectively, after the field variables have been established.

$$f_{avg} = \left(\Delta P_f D_{\text{hy}}\right) / \left(2\frac{L}{\cos\theta}\rho_f u_f^2\right)$$
 (6)

$$Nu_{avg} = (h_{avg}D_{hy})/(k_f)$$
 (7)

In microchannels, f_{avg} the average friction factor, ΔP_f (Pa) the pressure drop between the inlet and outlet, Nu_{avg} represents the average Nusselt number, h_{avg} (W/mK) the average heat transfer coefficient, and u_f is the average velocity within the microchannel. The microchannel's average heat transfer coefficient is obtained using equation (8).

$$h_{avg} = q''/LMTD = q''/\left[\frac{\left[\left(\overline{T}_{w,out} - \overline{T}_{f,out}\right) - \left(\overline{T}_{w,in} - \overline{T}_{f,in}\right)\right]}{\ln\left[\left(\overline{T}_{w,out} - \overline{T}_{f,out}\right) / \left(\overline{T}_{w,in} - \overline{T}_{f,in}\right)\right]}\right]$$
(8)

The LMTD is the log mean temperature difference represented by the fluid's inlet temperature $T_{f,in}$, the fluid's average outlet temperature $T_{f,out}$, the the temperature of the edges surface at the microchannel's inlet $T_{w,in}$ and

at its outlet $T_{w,out}$. The fluid used in the study is water and its thermophysical properties used are ($\rho_f = 1000 \text{ kg/m}^3$, $\mu_f = 0.001006 \text{ Pa.s}$, $k_f = 0.597 \text{ W/mK}$ and $C_{p,f} = 4181 \text{ J/kgK}$). In order to comprehend the impact of hydraulic diameter and Reynolds number, parametric studies are conducted for Reynolds numbers ranging from 100 to 500.

The model is based on a number of assumptions, including steady state operation, operating in a continuum regime, minimum viscous dissipation and external heat transfer, and no phase shift during flow. This work uses computational fluid dynamics without any changes because researchers have already proven the validity of the continuous regime relevant to flow in microchannels.

RESULTS AND DISCUSSION

Figure 2.a shows the heat transfer coefficient and pressure drop of triangular rib microchannels with Reynolds numbers between 100 and 500. The heat transfer coefficient is shown by the vertical axis on the left, while the pressure drop is shown by the vertical axis on the right. For triangular ribs microchannels, Figure 2.b illustrates the relation between the friction factor and Nusselt and Reynolds numbers across the same range of Reynolds numbers. The Nusselt number and friction factor are shown on the right and left vertical axes, respectively. Since it is expected that the triangle ribs microchannel has a higher pressure drop and heat transfer coefficient than the smooth microchannel, the friction factor and Nusselt number are higher than in microchannel with triangle ribs. The frequent disintegration of boundary layers and the appearance of secondary flows—flows that are perpendicular to the primary direction of flow—cause the heat transfer coefficient to increase at a given Reynolds number.

The temperature and velocity contours are shown at the middle of the microchannels' specified place with triangular rib surfaces at Re = 100, 300, and 500, respectively, in Figures 3, 4, and 5. Figure 6 shows the temperature contours for various Reynolds numbers (Re = 100, 500, and 500) at the specified site of the smooth-surfaced microchannel. It is evident that the temperature is highest at the lowest Reynolds number in both the triangle rib and smooth rib microchannels. It is also shown that the highest temperature is found near the two side surfaces and at the corners of the channel. When comparing the velocity profiles of the smooth and triangular ribs microchannels at comparable points along the microchannel's length in Figure 3, it is evident that the velocity boundary later continuously disturbed due the triangle ribs. As the Reynolds number rises, it is evident that the Nusselt number and the heat transfer coefficient also rise. This is a result of increased boundary layer disturbance and intensified secondary flows. A triangle ribs microchannel has a greater heat transfer coefficient and Nusselt number than a smooth microchannel at every Reynolds number taken into consideration in this work, and the difference increases with increasing Reynolds number.

2202 Alnaimat

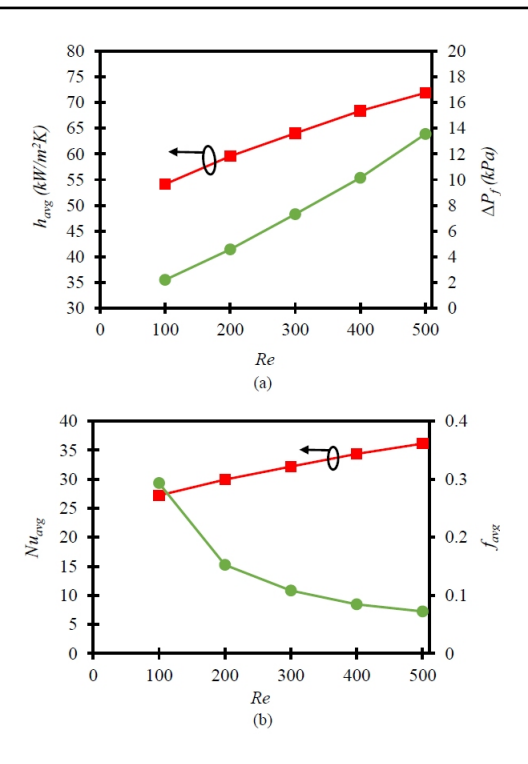


Figure 2: Thermal and hydraulic performance parameters (a) h_{avg} and ΔP with Re and (b) Nu_{avg} and f_{avg} with Re of triangle ribs microchannels (\blacksquare) h_{avg} or Nu_{avg} and (\bullet) ΔP or f_{avg} ($D_{hv} = 300 \ \mu m$, $L = 1 \ cm$).

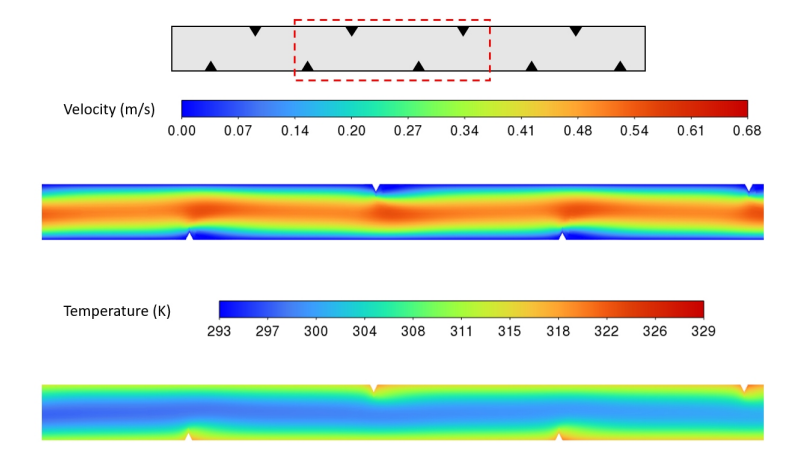


Figure 3: Velocity and temperature contour plot at location 1 of triangle ribs for Re = 100 ($D_{hv} = 300 \ \mu m$, $L = 1 \ cm$).

Because boundary layers are frequently disrupted and secondary flows are present in triangle ribs microchannels, the pressure drop associated with triangle ribs microchannels increases with increasing Reynolds number. For the same Reynolds number, the triangle ribs microchannel's friction is higher than the smooth microchannel's. It is found that the friction factor of triangular rib microchannels decreases as the Reynolds number rises.

The friction factor is directly related to the pressure drop and inversely proportional to the average flow velocity triangle. Even though both the pressure drop and average flow velocity increase with increasing Reynolds number, the observed decrease in friction factor with Reynolds number can be explained by the fact that the pressure drop increase with Reynolds number is less than the increase in flow velocity with Reynolds number.

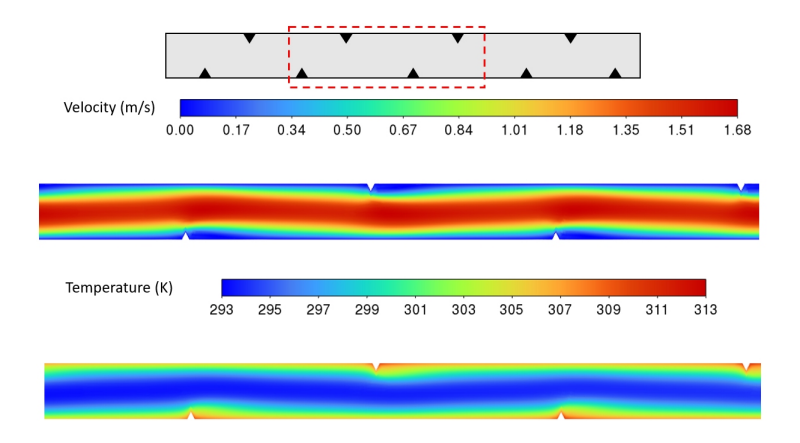


Figure 4: Velocity and temperature contour plot at location 1 of triangle ribs for Re = 300 (D_{hy} = 300 μ m, L = 1 cm).

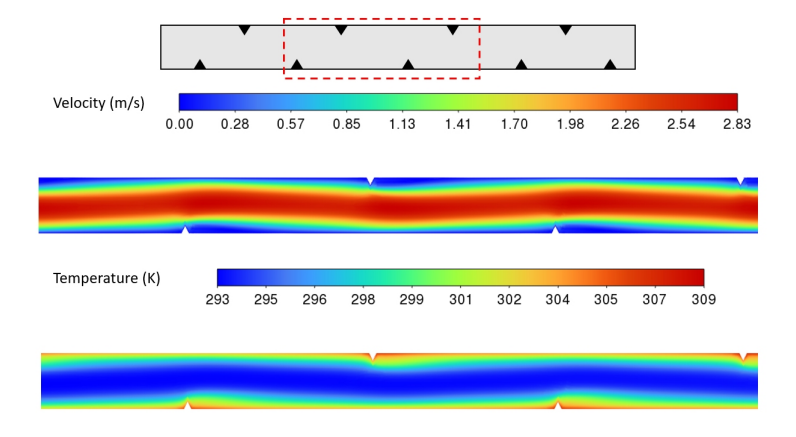


Figure 5: Velocity and temperature contour plot at location 1 of triangle ribs for Re = 500 (D_{hy} = 300 μ m, L = 1 cm).

2204 Alnaimat

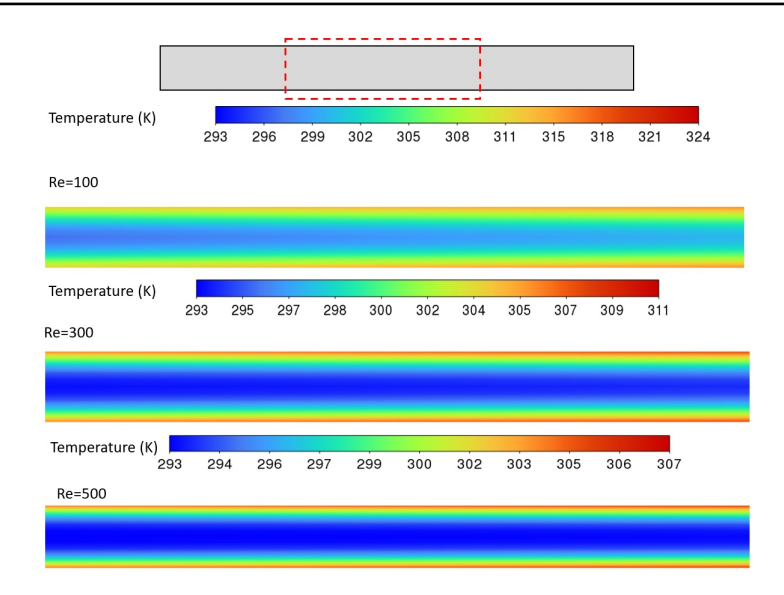


Figure 6: Temperature contour plot at location 1 of smooth channel for Re = 100, 300, 500 (D_{hv} = 300 μ m, L = 1 cm).

CONCLUSION

The thermohydraulic performance of triangle-ribbed microchannels under a steady heat flow was carefully examined in this work. The friction factor, Nusselt number, heat transfer coefficient, and pressure drop are used to analyse the performance in the region of 100 to 500 Reynolds numbers. It is discovered that microchannels with triangle ribs have higher friction factors, pressure drops, heat transfer coefficients, and Nusselt numbers than smooth microchannels. This study examines how the Reynolds number affects the functionality of a microchannel with triangle ribs and a smooth surface. An increase in Re is found to provide both a higher pressure drop and a higher heat transfer coefficient.

ACKNOWLEDGMENT

The authors acknowledge funding from United Arab Emirates University through grant (#12R231 and #12R127).

REFERENCES

Alnaimat, F, Ahmad Rahhal, Mathew, B., Fluid flow and heat transfer investigation of microchannel heat sink with sidewall triangle pin-fins, Int. J. of Thermofluids, 2025, 101141.

Alnaimat, F, Daadoua, M., Mathew, B., Effect of pin fins on heat transfer during condensation in minichannel heat exchanger, International Journal of Thermofluids, 2024, 100917.

Alnaimat F., El Kadi K., Mathew B., CFD investigation of R134a and Propane condensation in square microchannel using VOF model: Parametric study using steady state solution, Journal of Thermal Science and Engineering Progress, 2023, 38, 2451–9049.

- Alnaimat, F., Mathew, B. (2023) "Flow distribution in microchannel devices with U-shaped manifolds," International Journal of Thermofluids, vol. 19, p. 100391.
- Alnaimat F., Ziauddin M., Experimental investigation of Heat Transfer in Pin-fins heat sinks for cooling application, Journal of Heat and Mass Transfer, 2020, 1–7.
- Daadoua M., Mathew B., Alnaimat F., Experimental investigation of pressure drops and heat transfer in minichannel with smooth and pin fin surfaces, International Journal of Thermofluids, 2024, 21, 100542.
- El Kadi K., Alnaimat F., Sherif S. A, Recent advances in condensation heat transfer in mini and micro channels: A comprehensive review, Applied Thermal Engineering, 2021, 117412.
- Mathew, B. & Weiss, L. (2015), MEMS Heat Exchangers, in Materials and Failures in MEMS and NEMS, editors A. Tiwari and B. Raj, Scrivener Wiley, 63–120.
- Steinke, M. E. & Kandlikar, S. G. (2004), Review of Single-Phase Heat Transfer Enhancement Techniques for Application in Microchannels, Minichannels and Microdevices, International Journal of Heat and Technology, 22, 3–11.
- Sui, Y., Teo, C. J., Lee, P. S., Chew, Y. T., Shu, C. (2010), Fluid Flow and Heat Transfer in Wavy Microchannels, Int. Journal of Heat and Mass Transfer, 53, 2760–2772.
- Zheng, Z., Fletcher, D. F. & Haynes, B. S. (2013), Chaotic Advection in Steady Laminar Heat Transfer Simulations: Periodic Zigzag Channels with Square Cross-Sections, International Journal of Heat and Mass Transfer, 57, 274–284.
- Zheng, Z., Fletcher, D. F. & Haynes, B. S. (2013), Laminar Heat Transfer Simulations for Periodic Zigzag Semicircular Channels: Chaotic Advection and Geometric Effects, International Journal of Heat and Mass Transfer, 62, 391–401.